

OPEN ACCESS

Volume: 12

Special Issue: 1

Month: July

Year: 2024

P-ISSN: 2321-788X

E-ISSN: 2582-0397

Received: 28.05.2024

Accepted: 24.06.2024

Published: 10.07.2024

Citation:

Nitharsana, M and M. Indirani. "Encoding Anticancer Potential of Zingerone: Bioinformatic and Molecular Docking Analysis Targeting Liver Cancer." *Shanlax International Journal of Arts, Science and Humanities*, vol. 12, no. S1, 2024, pp. 127–51.

DOI:

<https://doi.org/10.34293/sijash.v12iS1-July.8025>

# Encoding Anticancer Potential of Zingerone: Bioinformatic and Molecular Docking Analysis Targeting Liver Cancer

**M. Nitharsana**

*Department of Biomedical Sciences  
Alagappa University  
Karaikudi, Tamil Nadu, India*

**M. Indirani**

*Department of Biomedical Sciences  
Alagappa University  
Karaikudi, Tamil Nadu, India*

## Abstract

*Liver cancer is the third-leading cause of cancer death globally, requiring research on molecular mechanisms for sustainable prevention and treatment. With expensive conventional drugs and severe side effects, novel medications are needed. Therefore, in the current investigation employing a bioinformatic approach, we explored the bioactive phytochemical zingerone for its anticancer efficacy targeting liver cancer. The study analyzed phytochemicals' drug-like nature using SWISS ADME, finding them orally available and meeting Lipinski, Ghose, Veber, Egan, and Muegge rules.*

*They showed good ADMET properties and strong interactions with apoptotic regulator target proteins, making them safe for commercial anticancer drugs. hGLUT, DDEFL1, HBx, BCL2, AFP, NF kappa, and Heat Shock Protein 70 Shows good binding affinity in the range of -5.3 to -6.0 kcal/mol. The phytocompound zingerone shows good binding affinity with all target proteins (-5.8 to -6.0 kcal/mol), thereby possessing appreciable bonded and non-bonded interactions with the binding pockets of target proteins. This study's findings could lead to the development of promising drug candidates for liver cancer, laying the foundation for the development of novel anticancer therapeutics.*

**Keywords: Liver Cancer, Pharmacokinetics, Drug Likeness, ADME Property, Molecular Docking, Zingerone.**

## **Introduction**

Liver cancer, primarily hepatocellular carcinoma (HCC), is a leading cause of cancer-related mortality worldwide, with the highest incidence rates observed in regions such as sub-Saharan Africa and Southeast Asia. It ranks as the sixth most common cancer and the third most common cause of cancer death, with approximately 750,000 new cases and over 700,000 deaths annually. HCC is strongly linked to chronic liver disease, particularly cirrhosis caused by hepatitis B virus (HBV) and hepatitis C virus (HCV) infections, alcohol abuse, and nonalcoholic fatty liver disease (NAFLD). Despite advances in medical science, conventional treatments, including surgical resection, liver transplantation, and systemic therapies, face significant limitations, including low response rates, high costs, and adverse side effects. These challenges underscore an urgent need for novel, more effective therapeutic options with improved safety profiles.

In recent years, attention has shifted towards natural compounds with bioactive properties, particularly those derived from medicinal plants. These compounds often possess diverse mechanisms of action, reduced toxicity, and have historically been valuable sources of new drugs. Zingerone, a phenolic compound isolated from ginger (*Zingiber officinale*), has garnered interest due to its diverse biological activities, including antioxidant, anti-inflammatory, and anticancer properties. Preliminary studies have shown that zingerone can inhibit cell proliferation, induce apoptosis, and suppress angiogenesis in various cancer models. However, its anticancer mechanisms, specifically against liver cancer, remain underexplored.

This study aims to investigate the anticancer potential of zingerone against liver cancer using a bioinformatics approach. Molecular docking was employed to analyze zingerone's binding affinity with several key proteins involved in liver cancer pathogenesis, such as human glucose transporter 1 (hGLUT1), hepatitis B virus X protein (HBx), B-cell lymphoma 2 (Bcl-2), and alpha-fetoprotein (AFP). Additionally, we assessed the compound's pharmacokinetics, drug-likeness, and toxicity profile through *in silico* ADME (Absorption, Distribution, Metabolism, Excretion) analysis and toxicity prediction tools.

The findings from this study offer insights into the potential of zingerone as a liver cancer therapeutic, highlighting its interactions with critical cancer-related proteins, favorable pharmacokinetic profile, and minimal toxicity. These results lay a foundation for further research and clinical validation of zingerone as a safe, cost-effective alternative in liver cancer treatment.

## **Materials and Methods**

### **Target and Ligand Preparation**

In this study, several target receptor molecules associated with liver cancer were selected, including human glucose transporter 1 (hGLUT1, PDB ID: 5EQG), Development and Differentiation Enhancing Factor-Like 1 (DDEFL1, PDB ID: 2B0O), hepatitis B virus X protein (HBx, PDB ID: 8GTX), B-cell lymphoma 2 (BCl2, PDB ID: 6ZX7), alpha-fetoprotein (AFP, PDB ID: 7YIM), nuclear factor kappa B (NF- $\kappa$ B, PDB ID: 1A3Q), and heat shock protein 70 (HSP70, PDB ID: 4PO2). These protein structures were obtained from the RCSB Protein Data Bank (Sussman et al., 1998). Each protein was prepared by removing water molecules and any non-standard residues, followed by the addition of missing hydrogens and charges to ensure proper conformation. The modified structures were saved in PDBQT format in the PyRx workspace for docking purposes. The structure of the phytochemical zingerone was sourced from the PubChem database and converted into PDBQT format using AutoDock tools to prepare it as a ligand for docking.

### **Molecular Docking**

Molecular docking was carried out using AutoDock Vina within the PyRx software. A rigid docking approach was applied to each protein receptor while allowing the ligand, zingerone, to remain flexible. This setup allowed us to evaluate the binding affinity and potential interactions between zingerone and each target protein. For each docking experiment, a conformational search was performed using the default settings of the Lamarckian genetic algorithm.

Grid parameters were adjusted to fully cover the ligand-binding site of each protein. The grid box dimensions were set to encompass the active site, with specific coordinates (X: 5.81, Y: 60.15, Z: 29.97) and box size values of 43.12, 35.86, and 58.03, respectively. This setup ensured that the binding interactions within the active site were accurately mapped. After docking, interactions such as hydrogen bonds,  $\pi$ - $\pi$  stacking, and hydrophobic interactions were analyzed using BIOVIA Discovery Studio Visualizer (v21.1.0.20298) (Kirubhanand et al., 2022).

During the molecular interaction study, active binding sites on each protein were predicted using the CASTp v3.0 server, with further identification of catalytic residues using the Firestar Server v58 based on prior studies. Phytocompounds that demonstrated favorable docking scores were advanced to the ADMET analysis phase for additional pharmacokinetic and toxicity assessments (Lopez et al., 2011).

### **Toxicity Prediction Using ProTox-II**

The ProTox-II tool was used to predict the toxicity profile of zingerone, leveraging a machine-learning model that forecasts toxicity based on chemical structure and physicochemical properties. ProTox-II provides a comprehensive toxicity profile that includes predictions for hepatotoxicity, organ toxicity, and oral toxicity. A key feature of ProTox-II is its in-depth analysis of adverse outcome pathways (AOPs), which helps to elucidate the molecular mechanisms behind potential toxic effects (Nachammai et al., 2023). SMILES strings, obtained from the PubChem database, were input into ProTox-II for toxicity evaluation. To further ensure accuracy, toxicity was

cross-verified using the STopTox tool, which provides detailed predictions of toxicity endpoints with visual fragment analysis (Borba et al., 2022).

STopTox, which uses QSAR models, allows direct SMILES input or structure drawing to generate toxicity predictions. It provides visual maps highlighting toxic and non-toxic fragments, with toxic regions shown in red and non-toxic regions in green (Riniker and Landrum, 2013).

### **Drug-Likeness and Pharmacokinetic Properties**

The drug-likeness of zingerone was evaluated using the SWISS ADME web server. This tool uses established rules, including Lipinski's rule of five, as well as criteria from Ghose, Veber, Egan, and Muegge, to assess drug-likeness based on molecular properties such as weight, hydrogen bonding, and topological polar surface area (TPSA). Only compounds with no rule violations were considered suitable for oral bioavailability and were subsequently assessed in the ADMET (Absorption, Distribution, Metabolism, Excretion, and Toxicity) analysis using PreADMET (Sindhu et al., 2023).

In the ADMET analysis, zingerone demonstrated favorable pharmacokinetic properties, including balanced lipophilicity (Log P) and high intestinal absorption (80.5–100%), indicating its potential for effective bioavailability. The compound's favorable aqueous solubility further supports its suitability for oral bioavailability, highlighting its potential utility in drug discovery and development.

## Results and Discussion

### Molecular Docking

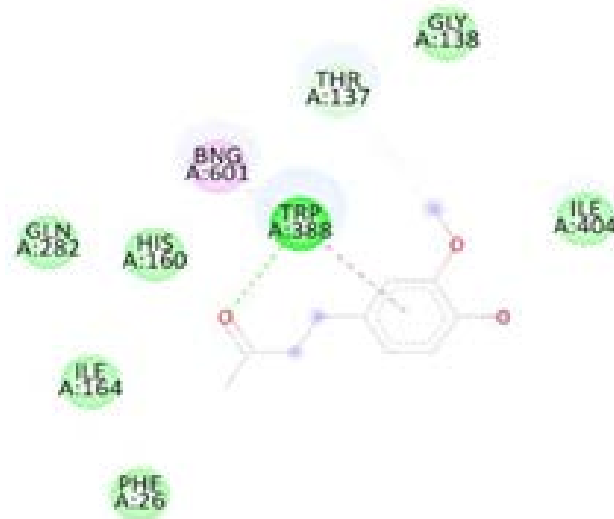
Molecular docking is a structure-based virtual screening approach that designs computerized medicines for specific ailments. It determines the binding orientation of ligands for their target molecules, through which the biological efficacy of phytochemicals can be predicted.

The binding affinity between targeted proteins, namely hGLUT [PDB ID:5EQG], DDEFL 1 [PDB ID:2B0O], HBx [PDB ID:8GTX], Bcl2 [PDB ID:6ZX7], AFP [PDB ID:7YIM], NF kappa [ PDB ID:1A3Q] and Heat Shock Protein 70 [PDB ID:4PO2]. The selected ligands were docked with the protein targets using AutodockVina (Version 4). The docking interactions of compound zingerone with the hGLUT [PDB ID: 5EQG] target molecule exhibited a binding affinity of -6.0 kcal/mol. The docking interaction of Zingerone with DDEFL 1 [PDB ID: 2B0O] The target molecule exhibited a binding affinity of -5.3 kcal/mol. The docking interactions of zingerone with HBx [PDB ID:8GTX], the target molecule, revealed a binding affinity of -5.9 kcal/mol, respectively. The docking interaction of the protein with Bcl2 [PDB ID: 6ZX7], the target molecule, revealed a binding affinity of -5.8 kcal/mol. The docking interaction of protein AFP [PDB ID: 7YIM] with the target protein exhibited binding at -6.0 kcal/mol. The docking interaction of zingerone with NF-kappa [ PDB ID:1A3Q] target protein exhibited a binding affinity of -5.8 kcal/mol. The docking interaction of zingerone with heat shock protein 70 [PDB ID: 4PO2] target protein exhibited a binding affinity of -5.8 kcal/mol. The top-scoring phytochemicals with receptors were further selected for the docking complex interactions. The results of interactions

between amino acid residues at the binding sites and the zingerone molecules revealed the participation of hydrogen and an alkyl bond.

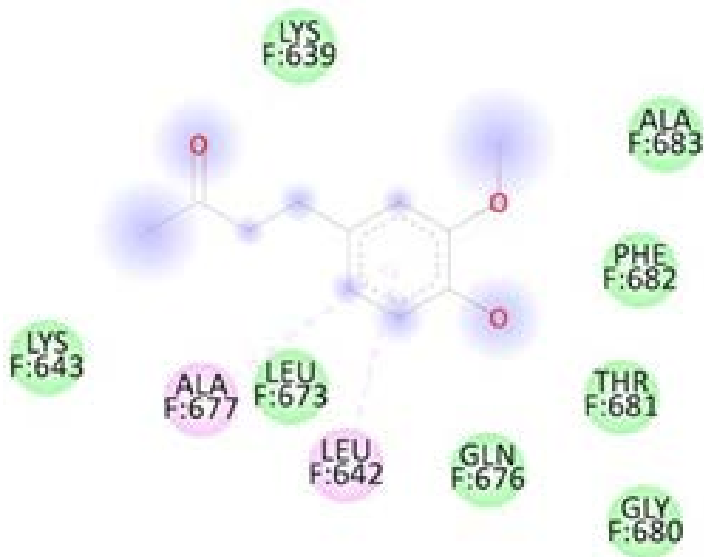
The interaction of zingerone with hGLUT reveals the four different types of interaction, such as Trp:151, which forms a pi-pi stacked, Bng:601, which forms a pi-alkyl, Thr137, which forms a Vanderwals, and Trp:388, which forms a conventional hydrogen bond. The interaction of zingerone with DDEFL1 reveals two interactions, such as Leu:642 and Ala:677, which form pi-pi alkyl bonds. The interaction of zingerone with HBx reveals three different types of interaction, such as Phe:141 forms. Pi-Pi is stacked, and Phe:141 forms Pi Alkyl, Trp:151 forms Pi-sigma. The interaction of zingerone with Bcl2 reveals four different types of interactions, such as Da:15 forms a conventional hydrogen bond, Dc:1 and Da:11 form Pi-Pi stacked, Dg:13 forms Pi anion, and Dc:1 forms a carbon hydrogen bond. The interaction of zingerone with AFP It reveals two different types of interactions, such as Gln:140, Arg:169, Phe:158, which form conventional hydrogen bonds, and Lys:161, Phe:158, which form alkyl bonds. The interaction of zingerone with NF Kappa reveals two different types of interactions, such as the Dc:612 form Pi anion bond. Dt:611 forms both a conventional hydrogen bond and a carbon hydrogen bond. The interaction of zingerone with heat shock protein 70 reveals four different types of interactions, such as Val:428 forms a pi-alkyl bond, Leu:439 forms a conventional hydrogen bond, and both Cys:533 and Val:414 form a pi-alkyl bond. Leu:522 forms a pi-sigma bond. (Kirubhanand et al., 2023).





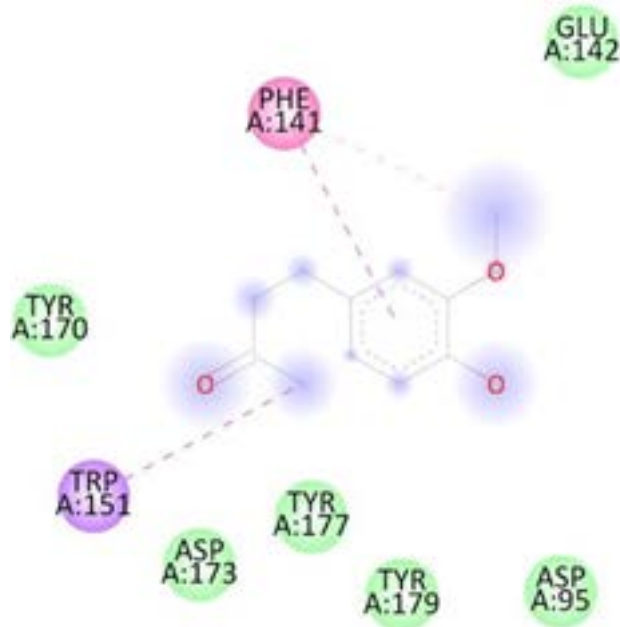
## Figure 1 a) Interaction Profiling between hGLUT and Zingerone

The above figure shows the interaction of zingerone with hGLUT reveals the four different types of interaction, such as Trp:151, which forms a pi-pi stacked, Bng:601, which forms a pi-alkyl, Thr137, which forms a Vanderwals, and Trp:388, which forms a conventional hydrogen bond.



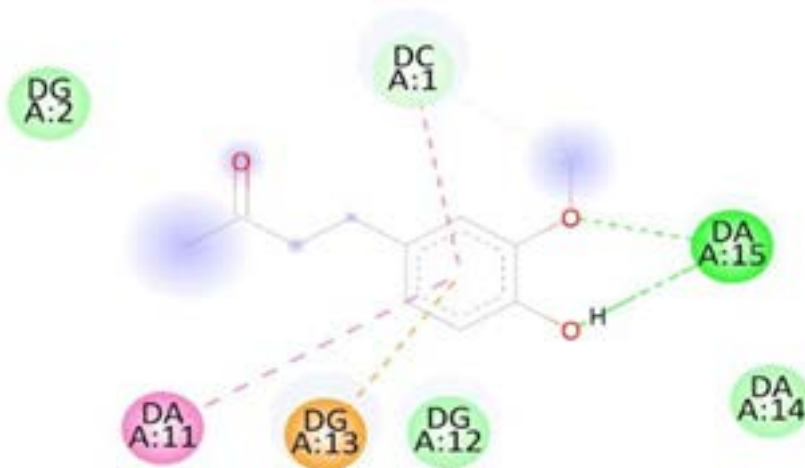
**Figure 1 b) Interaction Residues between DDEF1 and Zingerone**

The above figure shows the interaction of zingerone with DDEF1 reveals two interactions, such as Leu:642 and Ala:677, which form pi-pi alkyl bonds.



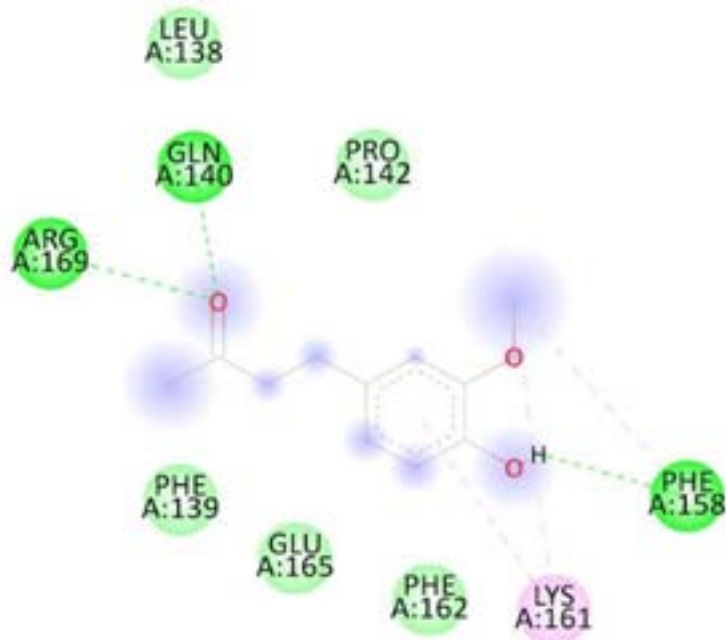
### Figure 1 c) Interaction Residues between Hbx and Zingerone

The above figure shows the interaction of zingerone with HBx reveals three different types of interaction, such as Phe:141 forms. Pi-Pi is stacked, and Phe:141 forms Pi Alkyl, Trp:151 forms Pi- sigma.



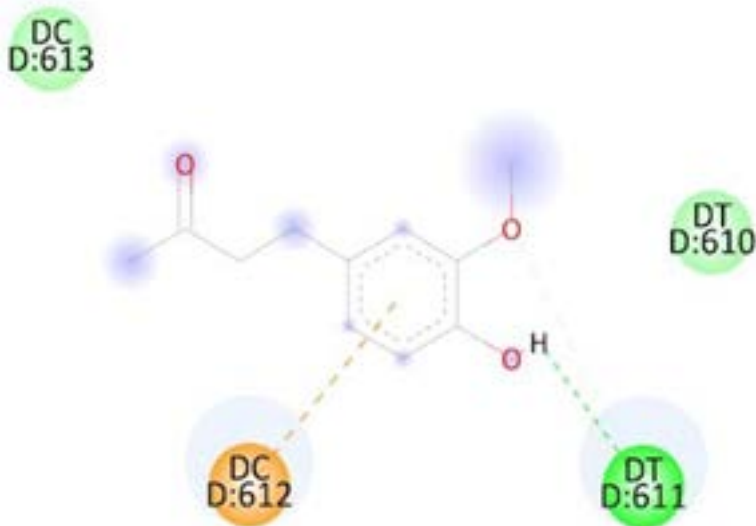
**Figure 1 d) Interaction Residues between Bcl 2 and Zingerone**

The above figure shows the interaction of zingerone with Bcl2 reveals four different types of interactions, such as Da:15 forms a conventional hydrogen bond, Dc:1 and Da:11 form Pi-Pi stacked, Dg:13 forms Pi anion, and Dc:1 forms a carbon hydrogen bond.



**Figure 1 e) Interaction Residues between AFP and Zingerone**

The above figure shows the interaction of zingerone with AFP. It reveals two different types of interactions, such as Gln:140, Arg:169, Phe:158, which form conventional hydrogen bonds, and Lys:161, Phe:158, which form alkyl bonds.



**Figure 1 f) Interaction Residues between NF Kappa and Zingerone**

The above figure shows the interaction of zingerone with NF Kappa reveals two different types of interactions, such as the Dc:612 form Pi anion bond. Dt:611 forms both a conventional hydrogen bond and a carbon hydrogen bond.



**Figure 7 g) Interaction Residues between Heat Shock Protein 70 and Zingerone**

The above figure shows the interaction of zingerone with heat shock protein 70 reveals four different types of interactions, such as Val:428 forms a pi-alkyl bond, Leu:439 forms a conventional hydrogen bond, and both Cys:533 and Val:414 form a pi-alkyl bond. Leu:522 forms a pi-sigma bond.

### **Toxicity Analysis of Zingerone**

In the therapeutic design phase, compound Zingerone is subjected to a detailed toxicity evaluation using the ProTox-II and STopTox servers. Toxic dosage determination was the main focus of the examination. The compound had no action in the pathways involved in stress response, nuclear receptor signaling, or organ toxicity. This means that dangerous qualities are either absent or dormant. Because of this, the lead compound

is considered non-toxic or to have no hazardous qualities because it does not show any negative effects. Table 1 provides an overview of the lead compound's toxicity prediction. Toxicity prediction clearly shows that the compound, zingerone, does not produce toxicity. (Nachammai et al., 2023)

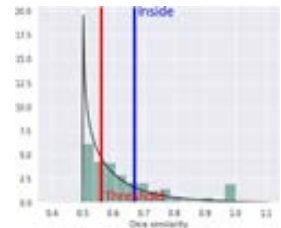

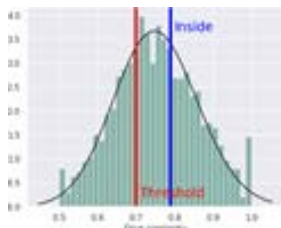

**Table 1 Prediction of Toxicity using ProTox-II Server for the Lead Compound**

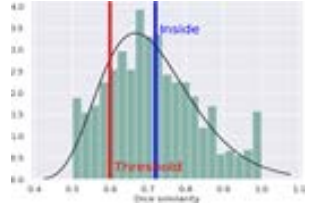
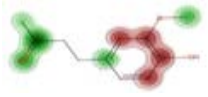
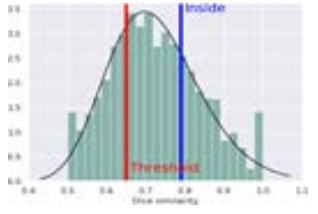

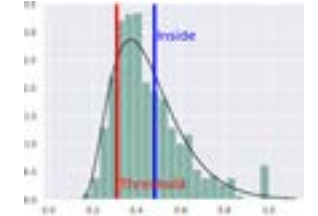

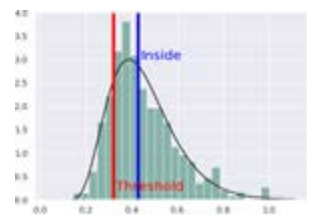

Classification	Toxicity	Zingerone
Organ toxicity	Hepatotoxicity	Inactive
	Carcinogenicity	Inactive
	Mutagenicity	Inactive
	cytotoxicity	Inactive
Tox21-nuclear receptor signaling pathways	Aryl hydrocarbon receptor (AhR)	Inactive
	Androgen receptor (AR)	Inactive
	Androgen receptor ligand binding domain (AR-LBD)	Inactive
	Aromatase	Inactive
	Estrogen receptor alpha (ER)	Inactive
	Estrogen receptor ligand binding domain (ER-LBD)	Inactive
	Peroxisome proliferator-activated receptor gamma (PPAR-Gamma)	Inactive
Tox21-stress response pathways	Nuclear factor (erythroid-derived 2)-like 2/antioxidant responsive element (nrf2/ARE)	Inactive
	Heat shock factor response element (HSE)	Inactive
	Mitochondrial membrane potential (MMP)	Inactive
	Phosphoprotein (Tumor Suppressor) p53	Inactive
	ATPase family AAA domain-containing protein 5 (ATAD5)	Inactive



Stoptox used to determine the expected contribution of each atom, this method examines the difference in the prediction of each bit that belongs to that atom. Then, the normalized contribution is used to color the atoms on a map that resembles topography. The structural pieces that are predicted to become a greater risk in each scenario are shown in red on these maps, while the fragments that are predicted to become less toxic are shown in green. Gray isolines define the boundary between the positive (red) and negative (green) contributions. Additionally, the majority vote of the random forest algorithm's internal models (the number of trees) determines the forecast certainty. The compound Zingerone was predicted for toxicity using stoptox (Table 2)

**Table 2 Prediction of Toxicity using Stoptox Server for the Lead Compound**

Toxicity	Applicability Domain (AD)	Predicted fragment contribution	score	prediction
Acute inhalation toxicity			73.0%	Non-toxic
Acute oral toxicity			90%	Non toxic

Acute dermal toxicity			64.0%	Non toxic
Eye irritation and corrosion			64.0%	Non toxic
Skin sensitization			60.0%	Non sensitizer
Skin irritation and corrosion			90%	negative

## Pharmacokinetics and Drug Likeness

To assess oral drug candidates on the basis of bioavailability, drug-likeness evaluates the molecules empirically based on their structural and physico-chemical characteristics. The pharmacological and pharmacognostic profile of the chosen phytochemicals is analyzed using the online SWISS ADME tool, which is based on five different rule-based filters: Lipinski, Ghose, Verber, Egan, and Mugge. To figure out if the phytochemicals enhance ADME and water-soluble features, drug similarity was evaluated. To determine if active compounds are orally active, Lipinski's rule of five is utilized as a technique

to assess the drug-likeness of the compounds. Pfizer's Lipinski filter uses physicochemical properties, such as molecular weight

<500 Da, MLOGP 5, number of rotatable bonds <10, and hydrogen atom count, to define tiny compounds. The physical properties, substructure presence, and functional groups of small compounds are described by the Ghose filter (Amgen). The range of criteria for tiny molecules includes the following: molar refractivity between 40 and 130, molecular weight between 160 and 480 Da, WlogP between -0.4 and +5.6, and total number of atoms between 20 and 70.

When the TPSA (total polar surface area) is equal to or less than 140 Å, the Veber filter (GSK filter) with 12 hydrogen bond donors and acceptors and a rotatable bond count of 10 indicates drug similarity. These compounds have strong oral bioavailability; higher rotatable bond counts are detrimental to the permeation rate; and lower TPSA is correlated with higher permeation rates. As it takes into consideration active transport and efflux pathways, the Egan computer model for human passive intestinal absorption (HIA) of small compounds is highly predictive of medication absorption. The TPSA and WLogP values, which are less than and equal to 131.6 and 5.88, respectively, 2000, serve as the foundation for Egan's rule. The numbers of rings are 7, carbon atoms > 4, heteroatoms > 1, rotatable bonds are 15, hydrogen bond acceptors are 10, and H-bond donors are 5, respectively.

The results for the assessment of the phytochemicals' drug-likeness were depicted in Table 3. The rate of drug permeability, or effective absorption through a biological barrier, is influenced

by molecular weight and TPSA. A pharmacological molecule's permeability decreases with increasing molecular weight and TPSA, and vice versa. Despite the fact that a drug's molecular weight is a major factor in its oral bioavailability, phytochemicals meet all the requirements and are thus considered excellent oral compounds. Compound bioavailability is correlated with TPSA; if a compound's TPSA value is less than 140Å, it can be readily absorbed in the gut, showing great oral bioavailability. The TPSA of the chosen phytochemicals was within the bounds set forth in the regulations. The number of rotatable bonds in the drug molecule determines its stereo-specificity, and the results are in good agreement (4 is acceptable) with all the phytochemicals. The Log P, TPSA, MW, HBA, and HBD values show the oral bioavailability of phytochemicals with strong membrane permeability as well as the hydrophobicity of medicinal molecules. Lipophilicity (Log P), which influences how well a medication molecule is absorbed by the body, is a significant factor. The absorption rate will decrease if the log P value is higher, and vice versa.

Every phytochemical in the current investigation is within the standard limit allowed by each regulation, indicating a higher rate of absorption. The quantity of hydrogen bond donors and acceptors should also fall within an appropriate range; if it does, the medication molecule's ability to permeate the cell membrane may be restricted. The phytochemical can pass through the cell membrane because the current study's result falls within the permitted limits.

The phytochemicals met the requirements of the Lipinski, Ghose, Veber, and Egan rules, and the drug-likeness study

therefore demonstrated that they have the potential to be orally bioavailable. The initial results offer an outline for the development of more effective and targeted anticancer medications. (Sindhu., et al., 2022).

**Table 3 Drug Likeliness Calculation for Phytocompound Zingerone**

Compound	Zingerone
Molecular weight	194.23
Heavy atoms	14
Rotatable bonds	4
H-bond acceptors	3
H-bond donors	1
Molar refractivity	54.53
Total polar surface area	46.53
XLOGP3	1.11
WLOGP	1.92
iLOGP	2.09
MLOGP	1.42
SILICOS-IT	2.41
No. atom. heavy atoms	6
Lipinski violation	0
Ghose violation	0
Veber violation	0
Egan violation	0

Bioavailability Radar offers a quick evaluation of a compound's drug-likeness. As can be seen, the pink area represents the ideal range for each parameter. To be deemed drug-like, a phytochemical's radar plot must fall within the pink area; as a result, the ligands are either predicted to be orally bioavailable or not by using the radar plot. Compounds' bioavailability is largely determined by two fundamental properties: polarity (polar) and flexibility (FLEX). (Mendie et al., 2022).



**Figure 7 ADME Prediction of Zingerone**

The above fig 7 shows Bioavailability Radar of the compound, zingerone's drug-likeness.

## Conclusion

Ginger, an essential spice, has chemopreventive effects through free radical scavenging, antioxidant pathways, gene expression alteration, and apoptosis, reducing tumor initiation, promotion, and progression. The compound zingerone from ginger spices shows anticancer activity. Accurately predicting the toxicity of an effective lead compound promotes further study and

improves lead optimization. In molecular dynamic simulations, it was discovered that the targeted protein-ligand complexes had strong hydrogen bond interactions that affected their stability and binding affinity. Thus, the study demonstrates the molecule from zingerone's potential as a liver cancer treatment alternative. Therefore, the research supports the identification and optimization of natural chemicals as a sustainable and financially viable means of advancing innovative therapeutics. The study found that zingerone, a molecule with the best features and minimal adverse effects, could be used for developing new therapeutic or preventative approaches against liver cancer. Thus, the knowledge gained by molecular docking provided insightful direction for subsequent drug development projects.

### **Abbreviation**

HCC : hepatocarcinoma

hGLUT : Human Glucose Transporter 1

DDEFL1 : Development and Differentiation Enhancing Factor-Like 1

HBx : Hepatitis B virus

Bcl2 : B-cell lymphoma-2

AFP : Alpha fetoprotein

NF Kappa B : Nuclear Factor Kappa B

ADME : Absorption, distribution Metabolism and Excretion

PDB : Protein Data Bank

### **Acknowledgement**

I would like to express my sincere gratitude to Alagappa University for providing the necessary laboratory facilities and resources that greatly supported the completion of this research.

## References

1. Allen, S.E., 2002. *The liver: Anatomy, Physiology, Disease and Treatment*. North Eastern University Press, USA.
2. Banerjee, P., Eckert, A.O., Schrey, A.K. & Preissner, R., 2018. ProTox-II: a webserver for the prediction of toxicity of chemicals. *Nucleic Acids Research*, 46(W1), pp.W257–W263.
3. Bielskutė, S., Plavec, J. & Podbevšek, P., 2021. Oxidative lesions modulate G-quadruplex stability and structure in the human BCL2 promoter. *Nucleic Acids Research*, 49(4), pp.2346–2356. doi:10.1093/nar/gkab057.
4. Borba, J.V., Alves, V.M., Braga, R.C., Korn, D.R., Overdahl, K., Silva, A.C., Hall, S.U.S., Overdahl, E., Kleinstreuer, N., Strickland, J., Allen, D., Andrade, C.H., Muratov, E.N. & Tropsha, A., 2022. STopTox: an in silico alternative to animal testing for acute systemic and topical toxicity. *Environmental Health Perspectives*, 130(2), p.027012. doi:10.1289/EHP9341.
5. Choi, J.S., Ryu, J., Bae, W.Y., Park, A., Nam, S., Kim, J.E. & Jeong, J.W., 2018. Zingerone suppresses tumor development through decreasing cyclin D1 expression and inducing mitotic arrest. *International Journal of Molecular Sciences*, 19(9), p.2832.
6. Groen, K.A., 1999. Primary and metastatic liver cancer. *Seminars in Oncology Nursing*, 15(1), WB Saunders.
7. Guyton, K.Z. & Kensler, T.W., 2002. Prevention of liver cancer. *Current Oncology Reports*, 4, pp.464–470.
8. Kapoor, K., Finer-Moore, J.S., Pedersen, B.P., Caboni, L., Waight, A., Hillig, R.C., Bringmann, P., Heisler, I., Müller, T., Siebeneicher, H. & Stroud, R.M., 2016. Mechanism of inhibition of human glucose transporter GLUT1 is conserved between cytochalasin B and phenylalanine amides. *Proceedings of the National Academy of Sciences of the United States of America*, 113(17), pp.4711–4716. doi:10.1073/pnas.1603735113.



9. Kirubhanand, C., Merciline Leonora, J., Anitha, S., Sangeetha, R., Nachammai, K.T., Langeswaran, K. & Gowtham Kumar, S., 2023. Targeting potential receptor molecules in non-small cell lung cancer (NSCLC) using in silico approaches. *Frontiers in Molecular Biosciences*, 10, p.1124563.
10. Kolluru, S., Momoh, R., Lin, L., Mallareddy, J.R. & Krstenansky, J.L., 2019. Identification of a potential binding pocket on viral oncoprotein HPV16 E6: a promising anti-cancer target for small molecule drug discovery. *BMC Molecular and Cell Biology*, 20(1).
11. Lopez, G., Maietta, P., Rodriguez, J.M., Valencia, A. & Tress, M.L., 2011. firestar — *Advances*.
12. Mendie, L.E. & Hemalatha, S., 2022. Molecular docking of phytochemicals targeting GFRs as therapeutic sites for cancer: an in silico study. *Applied Biochemistry and Biotechnology*, 194(1), pp.215–231.
13. Mondal, D., Das, K. & Chowdhury, A., 2022. Epidemiology of liver diseases in India. *Clinical Liver Disease*, 19(3), pp.114–117.
14. Nachammai, K.T., Amaradeepa, S., Raageshwari, S., Swathilakshmi, A.V., Poonkothai, M. & Langeswaran, K., 2023. Unraveling the interaction mechanism of compounds from *Cladophora* sp to recognize prospective larvicidal and bactericidal activities: in vitro and in silico approaches. *Molecular Biotechnology*, pp.1–21.
15. Otto, T. & Sicinski, P., 2017. Cell cycle proteins as promising targets in cancer therapy. *Nature Reviews Cancer*, 17, pp.93–115.
16. Ozougwu, J.C. & Eyo, J.E., 2014. Hepatoprotective effects of *Allium cepa* extracts on paracetamol-induced liver damage in rat. *African Journal of Biotechnology*, 13(26), pp.2679–2688.
17. Peck-Radosavljevic, M., 2014. Drug therapy for advanced-stage liver cancer. *Liver Cancer*, 3(2), pp.125–131.